Research Journal of Physical Sciences ISSN 2320–4796
Vol. **11(2),** 9-18, August **(2023)** *Res. J. Physical Sci.*

Study of the physical and mechanical properties in volume of TiN by the MEAM method

Yahnn Jeancy MIGHENSLE MIMBOUI[1,2,4*], Alain Second DZABANA HONGHELET[1,2,4] and Timothée SONGO[1,2,3]
[1]Faculty of Science and Technology, Marien Ngouabi University, Congo Brazzaville
[2]Research Group on Physical and Chemical Properties of Materials, Congo Brazzaville
[3]Geological and Mining Research Center, Congo Brazzaville
[4]Association Alpha Sciences Beta Technologies, Congo Brazzaville
mimbouiyahnn@gmail.com

Available online at: www.isca.in, www.isca.me
Received 25th March 2023, revised 8th July 2023, accepted 30th July 2023

Abstract

We present in this work the results of our study on the physical and mechanical properties of TiN. This work consisted in determining the physical and mechanical properties of the different crystallographic structures (B1, B2 and B3) of TiN using the MEAM (Modified Embedded Atom Method) as well as the MEAM potentials of titanium and nitrogen. We used the calculation code LAMMPS, based on classical molecular dynamics, to determine the most stable structure of TiN which remains the B1 structure with the crystal parameter a=4.24 A°, stable structure verified by the mechanical stability relation, for the cubic structure, given by the relation $C_{11} - C_{12} > 0$, $C_{11} > 0$, $C_{44} > 0$, $C_{11} + 2C_{12} > 0$. *The elastic constants found also allowed us to evaluate the anisotropy of the cubic system of TiN, the directions [110] and [111] are anisotropic in terms of wave progation velocity, unlike the one on the direction [100] whose propagation velocity remains the most important. The results obtained in this study were compared with the theoretical results and show considerable agreement.*

Keywords: MEAM, LAMMPS, Molecular Dynamics, Elastic Constants, Elastic Modules, Ovito, titanium nitride, debye temperature, anisotropy.

Introduction

Titanium nitride is a chemical compound with the formula TiN. It is a very hard and corrosion resistant ultra-refractory ceramic. It is used as a coating in mechanical engineering and remains an important area of application to increase the service life of cutting tools and their working performance. These tools are generally coated with a protective layer of TiN to improve wear and abrasion resistance, hardness, chemical stability, coefficient of friction and thermal conductivity for faster heat removal. Titanium nitride is also very commonly used in microelectronics where the miniaturization of electronic devices to nanometric dimensions requires the use of diffusion barriers[1-4]. Indeed, the metallization of integrated circuits and MOS (Metal Oxyde Semiconductor) transistors is generally ensured by aluminum and copper deposits, because of their excellent electrical conductivity and their good adhesion on SiO2. In order to prevent diffusion between these metals and the silicon, during the development or use, it is necessary to interpose an anti-diffusion barrier generally consisting of refractory metal nitride[5-7].

Due to its very good electrical conductivity, adhesion and chemical stability, titanium nitride is an ideal material[8]. These properties are also exploited in the design of other electronic devices such as gate electrodes in MOS transistors, low-barrier Schottky diodes and many other applications where silicon is used as a substrate[9].

It is also worth mentioning the use of titanium nitride as an anti-gas diffusion barrier for ultra-high vacuum chambers where TiN deposits allow to reduce the hydrogen permeability and thus improve the ultimate vacuum[10].

Finally, the optical properties of TiN are exploited for the selective transmission of light but also for aesthetic and decorative reasons. Since stoichiometric titanium nitride has a golden yellow color, it is widely used in jewelry where it replaces gold[11,12]. Its high resistance to scratching and corrosion are additional advantages[13].

Titanium nitride has a face-centered cubic structure (space group 225/Fm^{3}m, mesh parameter equal to 4.24 Å)[14]. It belongs to the class of interstitial nitrides, i.e. the nitrogen atoms occupy preferentially the octahedral interstitial sites of the metal crystal (titanium here). This structure, namely δ-TiN, is stable at high temperatures (T_{fusion}=2950°C) Professor Nsongo Timothée made a study of the structure and adhesion of thin layers of titanium and titanium nitride prepared by sputtering. He also characterized the adhesion of titanium and titanium nitride on the different substrates used by the "scratch" method in order to relate the growth conditions and the resulting structural characteristics to the adhesion[15].

Stéphane GROSSO has worked on Ti, TiN and TiOx architectural coatings developed by sputtering on stainless steel

wires. The main objective of his thesis was to understand the effects of the architecture of the deposits and of the elaboration parameters on the physicochemical characteristics of Ti, TiN and TiOx coatings and thus on their properties of use[16].

MERIEM Fodil, AMINE Mounire et al have worked on the structural and elastic properties of TiN and AlN compounds by studying first principles. Their work showed that the structural transition at 0°K from B1 structure (CFC type NaCl) to Wurtzite phase (B4) for TiN occurs at -26.34GPa and from wurtzite phase to B1 occurs at 10.48GPa for AlN[17].

This work is a simulation conducted under the Lammps code based on the Modified Embedded Atom Method and using MEAM potential.

Methodology

We performed a simulation under the LAMMPS code version 2020 with the executable lmp_mpi, under the Windows operating system, using the MEAM potentials found in the database at https://www.ctcms.nist.gov/potentials/system.

The MEAM potentials of titanium, nitrogen, and titanium nitride used in this work were developed by Y. M. Kim and B. J. Lee[18] whose parameters are aligned in the Table-1,2.

These potentials were used to calculate the cohesive energies under different crystallographic structures using the MPCV4 software. The calculations were simulated for periodic crystallographic structures for the 5x5x5 mesh under the calculation code lammps.

The different crystallographic structures studied in this work are: the B1 structure of the NaCl type, the B2 structure of the CsCl type as well as the B3 structure of the cubic ZnS type.

The input files allowed us to illustrate the different crystallographic structures through several visualization tools.

Table-1: MEAM parameters of Ti, N and TIN.

Parameters	Ti	N	TiN
Rc (A°)	4.8	4.6	4.6
Delr	0.1	0.1	0.1
Augt1	0	1	0
Erose_form	2	0	2
Ialloy	2	2	2
zbl (1,1)	0	1	0
Nn2 (1,1)	1	0	1
Rho0 (1)	1.00	1.00	18
Ec (1,1)	4.870	4.880	6.615
Re (1,1)	2.920	1.10	2.121
Alpha (1,1)	4.71945	4.330	5.092
Repuls (1,1)	0.00	0.00	0.00
Attrac(1,1)	0.00	0.00	0.00
Cmin(1,1,1)	1.00	2.00	0.16
Cmax(1,1,1)	1.44	2.80	2.80

Table-2: Complementary parameters of titanium and nitrogen**.**

elt	atwt	alat	β_0	β_1	β_2	β_3	t_0	t_1	t_2	t_3	esub	asub	α	Z	lat	ibar	rozero
Ti	47.88	2.92	2.7	1.0	3.0	1.0	1.0	6.8	-2.0	-12.0	4.87	0.66	4.71	12	hcp	3.0	1 .0
N	14.00	1.10	2.75	4.0	4.0	4.0	1.0	0.05	1.0	0.00	4.88	1.80	5.96	1	Sun	3.0	18

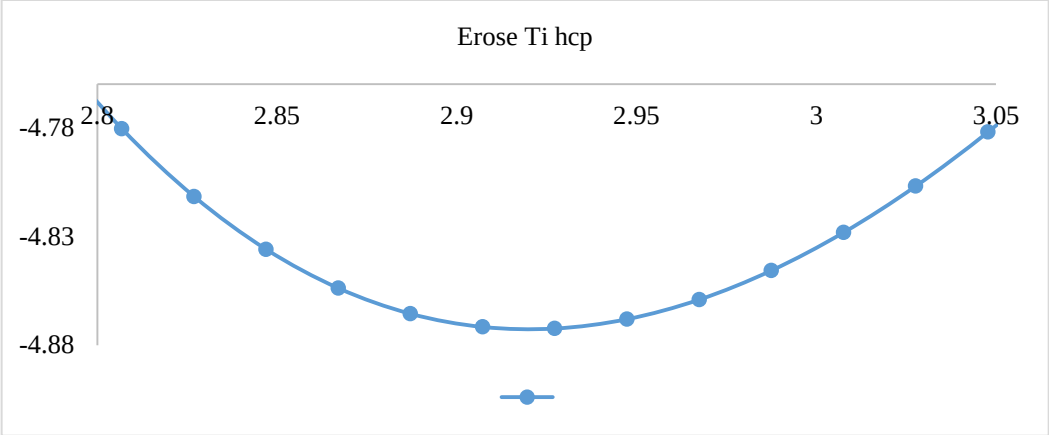

Figure-1: Rose energy of Titanium.

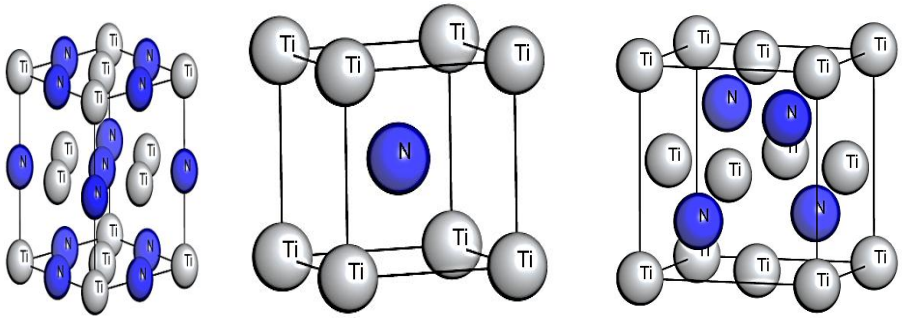

(a) (b) (c)

Figure-2: Different crystallographic structures of TiN: a) B1(NaCl) b) B2 c) B3.

Results and Discussion

In the following paragraphs we present the results obtained under the LAMMPS code using the MEAM potentials. These results were also calculated by the MPCV4 application under Windows 10, 64 bits. The crystalline parameters, elastic constants and moduli translating the structural stability for different TiN structures are presented in Table-3,4 and Figure-3,4.

Crystalline parameters: The presented crystal parameters and volumes have been calculated for the structures B1(NaCl), B2(CsCl), B3(ZnS) and are presented in Table-3. The most voluminous structure is the B3(ZnS) structure followed by the B1(NaCl) structure and finally the B2(CsCl) structure.

Table-3: Crystal parameters by structure and crystallographic volume.

Structures	a (Å)	b (Å)	c (Å)	Volumes (Å)^3
B1(NaCl)	4.24	4.24	4.24	76.23
B2(CsCl)	2.68	2.68	2.68	19.25
B3(ZnS)	4.54	4.54	4.54	93.58

Cohesive energy: We calculated the cohesive energies in different crystallographic structures for titanium nitride TiN; we realized that structure B1(NaCl) is the most stable with a cohesive energy of -6.62eV followed by structure B3(ZnS) with a cohesive energy of -5.97eV.

Table-4: Cohesive energy by structure.

Structures	Parameters (Å)	Total energy (ev)	Ecoh(ev)	Number of atoms
B1(NaCl)	4.24	-52.92	-6.62	8 (More stable)
B2(CsCl)	2.68	-11.53	-5.77	2
B3(ZnS)	4.54	-47.78	-5.97	8

The evolution of the cohesion energy per structure is represented in Figure-3,4. We notice that the number of atoms in the TiN structure plays an important role in the sense that the more the atoms increase the more stable the structure is.

Although the number of atoms per cell increases in some structures, the cohesion energy becomes very large, reflecting the instability of the structure beyond eight (8) atoms per cell.

The structures B1 and B3 are very close, although having the same number of atoms they present very close cohesive energies as well as the mesh parameters.

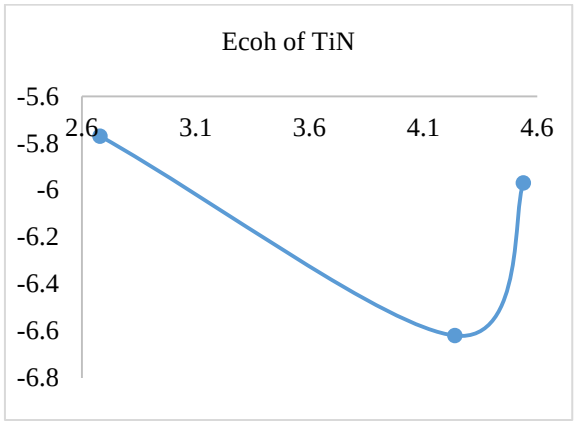

Figure-3: Evolution of the cohesive energy by crystal structure of TiN.

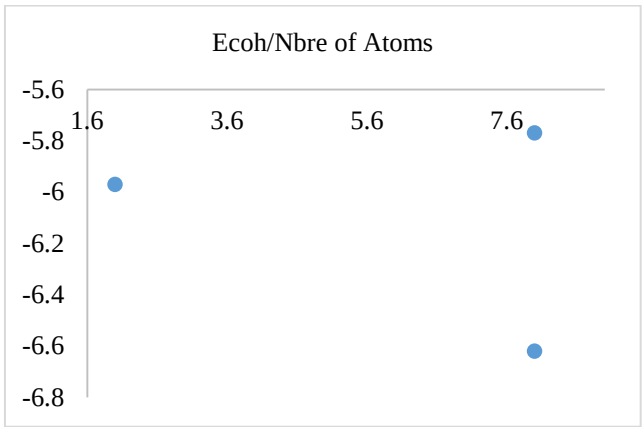

Figure-4: Evolution of the cohesive energy per atomic number of TiN.

The MEAM potential of TiN allowed us, thanks to the MPCV4 application, to represent the cohesion energies for different structures as shown in the Figure-5.

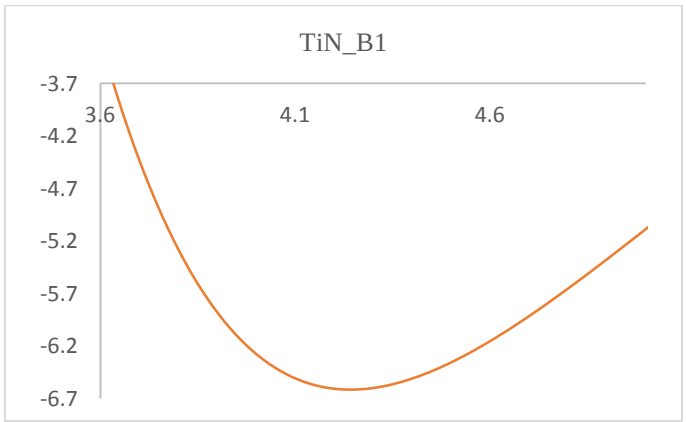

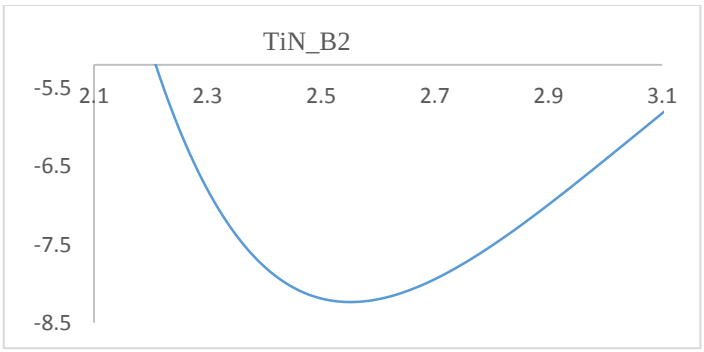

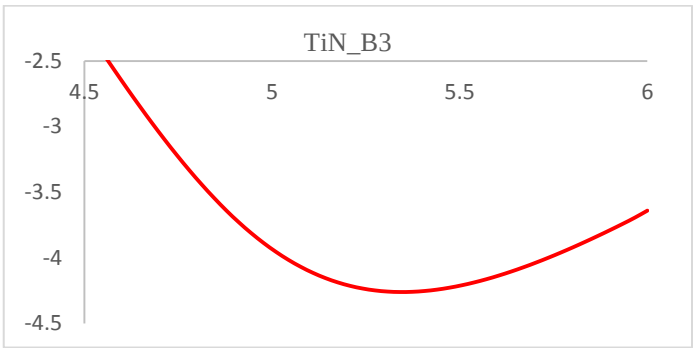

Figure-5: Pink energy of titanium in structure: a. B1 b. B2 c. B3.

Mechanical properties: We have calculated for the temperature of 298°K, the elastic constants of TiN under three different structures B1, B2 and B3 as well as the corresponding elastic moduli.

Elastic constants: The elastic constants C_{ij} are essential parameters for predicting the elastic properties and mechanical stability of materials[19,20]. The elastic and mechanical properties of solids reflect their reactions to the intervention of certain external factors. In the simplest case such factors are mechanical actions: compression, traction, bending, shock, torsion. In addition to mechanical actions, they can be thermal, magnetic, etc... These properties are determined, in the first place, by the forces of bonds which intervene between the atoms or the molecules constituting a solid.

When subjected to a stress, a crystal deforms linearly with respect to this stress as long as the deformation generated is small. When the stress is removed, the material returns to its standard state reversibly. This behavior observed for all materials is called "elastic".

In order to understand the mechanical stability, we studied the elastic constants at room pressure of TiN for three different structures such as NaCl (B1), CsCl (B2) and ZnS(B3). The cubic system is characterized by three independent elastic moduli: *C11*, *C12* and *C44*.

The elastic constants are determined by the stress-strain method based on Hooke's general law[21,22].

For elements that have a cubic structure, the criterion for predicting structural stability is as follows:

$C_{11} - C_{12} > 0$, $C_{11} > 0$, $C_{44} > 0$, $C_{11} + 2C_{12} > 0$

The cubic system is characterized by three independent moduli of elasticity: *C11*, *C12* and *C44*, and the *Cij* matrix can be written as: i. The constant C_{11} is the measure of the resistance to deformation produced by a stress applied to the (100), (010) and (001) planes along the <100> directions (length elasticity). ii. C_{44} represents the measure of resistance to deformation in the case of a shear stress applied on the (100), (010) and (001) planes along the diagonals (shape elasticity). iii. C_{12} has no simple physical interpretation, but these linear combinations with C_{11} give us the compressive modulus *B* and the shear modulus *G*.

$$C_{ij} = \begin{bmatrix} C_{11} & C_{12} & C_{12} & 0 & 0 & 0 \\ C_{12} & C_{11} & C_{12} & 0 & 0 & 0 \\ C_{12} & C_{12} & C_{11} & 0 & 0 & 0 \\ 0 & 0 & 0 & C_{44} & 0 & 0 \\ 0 & 0 & 0 & 0 & C_{44} & 0 \\ 0 & 0 & 0 & 0 & 0 & C_{44} \end{bmatrix}$$

The elastic constants for TiN structures B1, B2 and B3 were calculated and are presented in the Table-5.

By performing this calculation on the elastic constants of the TiN alloy in three structures B1, B2 and B3, we found that only structure B1 which has theoretical and experimental data and our computer simulation results are consistent with the literature. In conclusion, the most stable structure is B1.

The exploitation of these data allowed us to compare the elastic constants between them and between the theoretical and experimental data that we represent through, with series 1 for B1 and series 2 for B2 and series 3 for B3 (Figure-6,7).

The order of magnitude is well defined by $C_{11} > C_{12}$ and is preserved in the theory as well as for experimental data.

Comparing the data, we find that the elastic constants are in the same order of magnitude as the experimental data.

Elastic modules: In this paragraph we present the corresponding elastic moduli in different Reuss Hill and Voigt systems.

These moduli translate the rigidity and flexibility of the material, against external excitations; they translate the directions of the resulting deformation or the resulting stress. We also speak of elastic coefficients which are none other than the moduli of the engineer for the properties of nanomaterials, we give here the mathematical relationships between Young's modulus, compression, Poisson's ratio and shear with the elastic constants. i. The modulus of compression B is defined as the ratio of the hydrostatic pressure to the fractional change in volume produced by that pressure (the volume elasticity). ii. The second modulus *G* is the resistance to deformation produced by a shear stress applied to the plane (110) along the direction [110]. iii. The elastic moduli (Bulk modulus B, Shear modulus G and Young's modulus E) are estimated by the Voigt-Reuss-Hill method. Generally, the larger the B, the greater the resistance of the material to change in volume. iv. The elastic anisotropy A^U plays a vital role in the physical/mechanical process such as fracture behavior and phase transformations[25]. It can be deduced from the universal anisotropy index whose formula is as follows[26]: $A = {}^{U} 5\frac{G_v}{G_R} + \frac{B_v}{B_R} - 6$

Where: G_v and G_R represent the shear modulus of Voigt and Reuss, B_v and B_R are the Voigt and Reuss bulk modulus.

The set of elastic moduli in different systems of approaches for a cubic crystallographic structure are present in Table-6 [27]. The results obtained from the expressions of the previous modules are presented in Table-7.

Table-5: Elastic constants comparison with theory and experiment.

Elastic constants of TiN structures B1, B2 and B3 (GPa)									
Elastic moduli	Our work			Theory[23]			Exp.(298°K)[24]		
	B1	B2	B3	B1	B2	B3	B1	B2	B3
C11	602	486.19	279.81	610	-	-	625	-	-
C12	135	116.24	121.39	137	-	-	165	-	-
C44	153	25.19	91.03	158	-	-	163	-	-

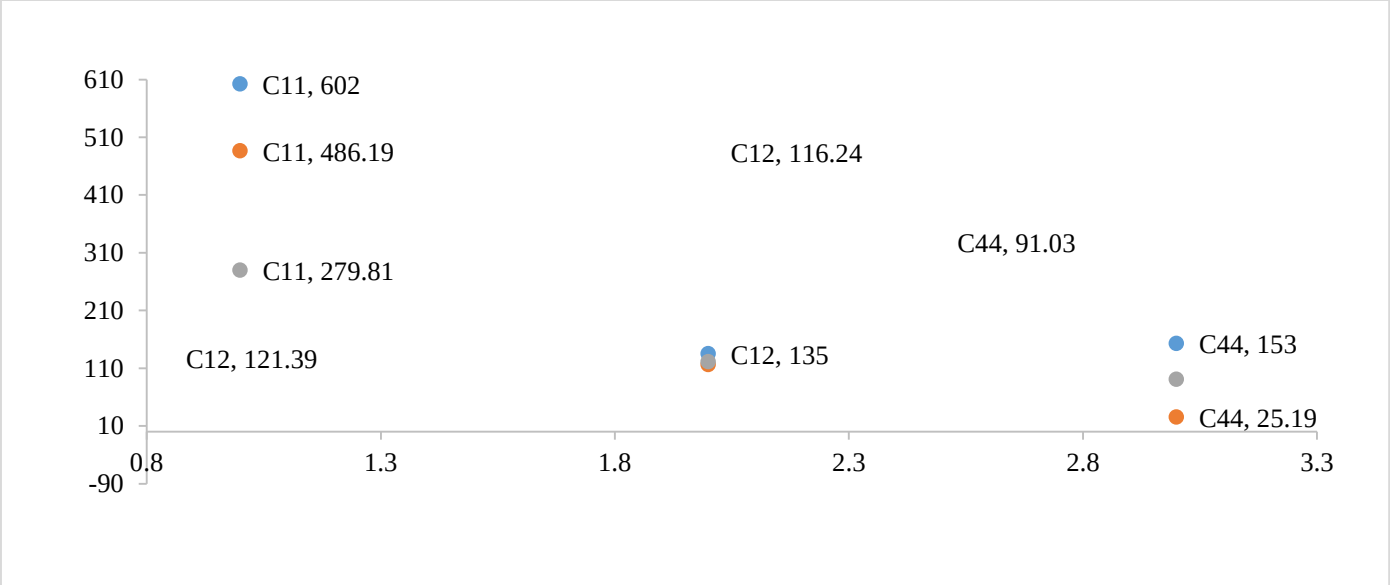

Figure-6: Elastic constants of the B1 B2 B3 structures of TiN.

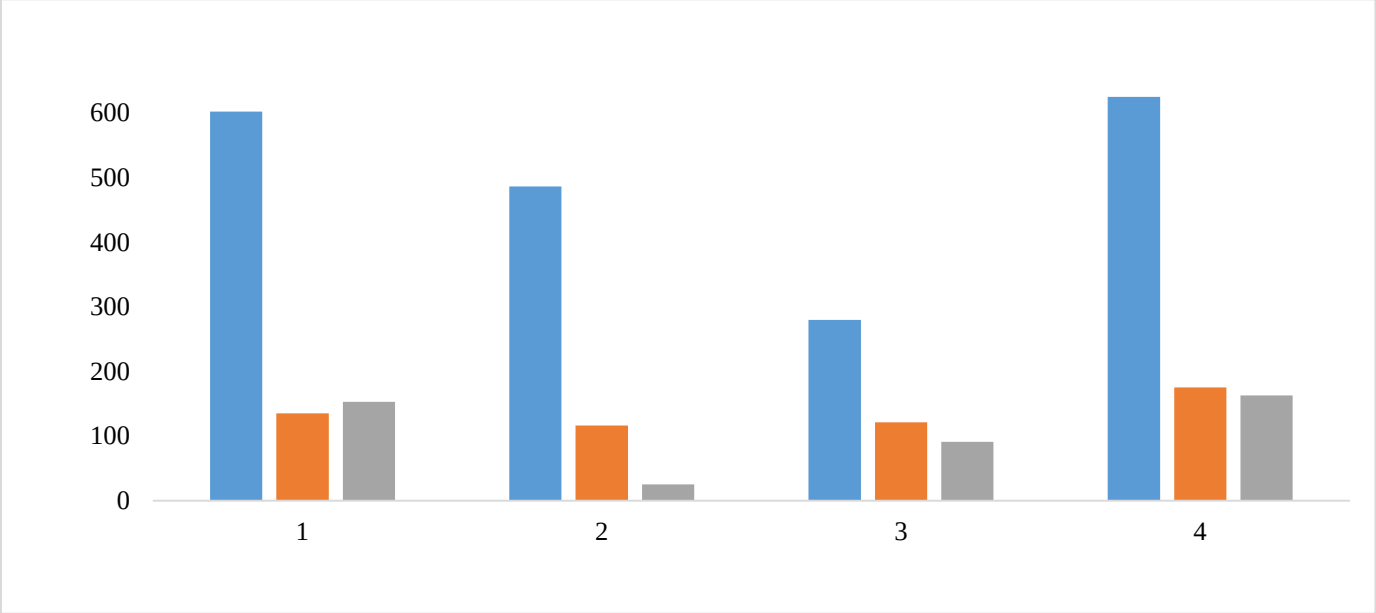

Figure-7: Order of magnitude comparison with experimental data(4).

Table-6: Mathematical expressions of elastic moduli for a cubic structure.

$E = \frac{9BG}{3B + G}$	$\nu = \frac{3B - E}{6B}$	$B = \frac{C_{11} + 2C_{12}}{3}$
$G_v = \frac{C_{11} - C_{12} + 3C_{44}}{5}$	$G_R = \frac{5(C_{11} - C_{12})C_{44}}{4C_{44} + 3(C_{11} - C_{12})}$	$G = \frac{G_R + G_V}{2}$
$B_{Hill} = \frac{1}{2}(B_{Reuss} + B_{Voigt})$	$B_R = B_R = \frac{1}{3}(C_{11} + 2C_{12})$	$G_{Hill} = \frac{1}{2}(G_{Reuss} + G_{Voigt})$

Table-7: Elastic Modules.

Elastic modules (Gpa) of B1, B2 and B3										
Size	Symbols	Voigt			Reuss			Hill		
		B1	B2	B3	B1	B2	B3	B1	B2	B3
Bulk modulus	B	256.09	239.56	174.19	256.09	239.56	174.19	256.09	239.56	174.19
Shear modulus	G	193.45	89.10	86.30	187.36	38.48	85.90	190.41	63.79	86.10
Young modulus	E	463.62	237.82	222.20	451.89	109.58	221.32	457.77	175.77	221.76
Elastic anisotropy	A^U	B1= 0.1625		B2= 0.01765		B3= 0.0232		-		
Fish ratio	V	0.1982	0.3345	0.2874	0.2059	0.4237	0.2882	0.2020	0.3777	0.2878

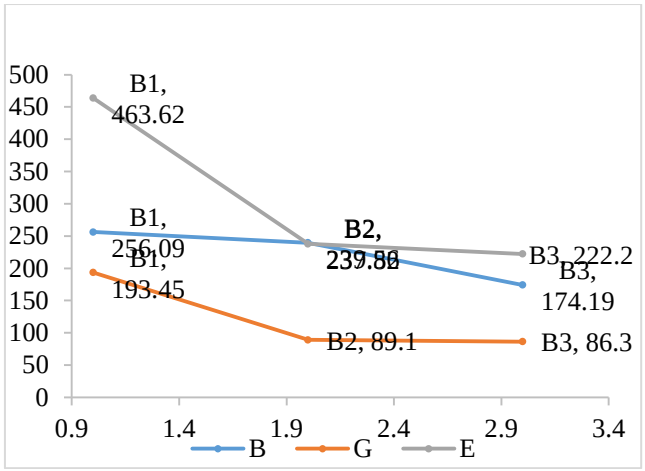

Figure-7: Modules according to the timestep.

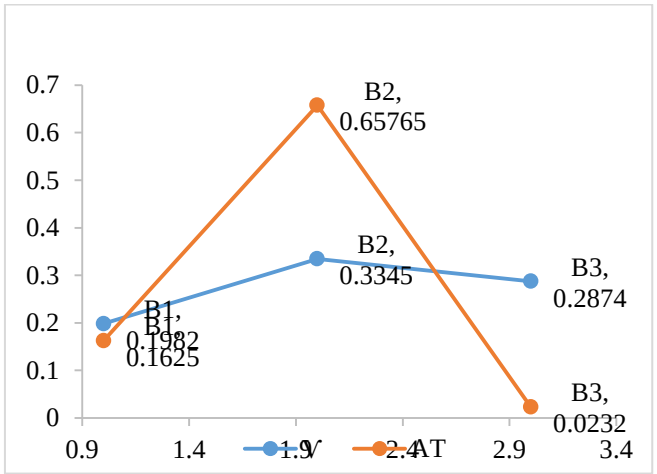

Figure-8: Modules according to the order parameter.

Thermodynamic properties: Debye temperature and wave propagation speed: The Debye temperature is a very important parameter for a solid. It is associated with thermodynamic properties of materials such as entropy, thermal expansion, and internal vibrational energy.

In this paragraph we present the results for the Debye temperature and the wave propagation velocities in the [100], [110] and [111] directions.

Once we have calculated the Young's modulus E, the stiffness modulus B and the shear modulus G, we can obtain the Debye temperature θ_D which is a parameter of fundamental importance closely related to several physical properties such as the heat of heat and the melting temperature.

A standard method for calculating the Debye temperature from the elastic constants is the formula that relates the average elastic wave velocity Vm and θ_D given by the following relation[27].

$$\theta_D = \frac{h}{k}\left[\frac{3n}{4\pi}\left(\frac{N_a\rho}{M}\right)\right]^{1/3} V_m$$

$$V_m = \left[\frac{1}{3}\left(\frac{2}{V_t^3}+\frac{1}{V_l^3}\right)\right]^{-1/3}$$

$$V_t = \left(\frac{G}{\rho}\right)^{1/2}$$

$$v_l = \left(\frac{3B+4G}{3\rho}\right)^{1/2}$$

M: molar mass. ρ: density, Na : Avogadro number. n: atomic number. h: Planck's constant. k: Boltzmann constant. $_D$: Θ Debye temperature

The results are presented in Table-8.

Table-8: Debye temperature and propagation speed.

Physical Properties	Values		
	B1	B2	B3
Bulk modulus (GPa)	256.09360	239.56729	174.19235
Compressibility (1/GPa)	0.00390	0.00417	0.00574
Elastic Debye temperature K	919.49812	483.09285	651.96894
Averaged sound velocity (m/s)	6568.30255	3399.06171	5046.81698
Density ρ $(g/cm)^3$	5.395	5.343	4.392

The calculated Debye temperature is around 558.56408K, this value is close to the one found by Xing Liu and Hui-Qing Han.

Wave propagation speed: We have calculated the velocities of propagation of the wave in a longitidunal way Vp, following the compression Vp, thermal vm.

The velocity relationships are given by the following expressions:

$$v_s = \sqrt{\frac{G_i}{\rho}}\ ; v_p = \sqrt{\frac{B_i + 4G_i/3}{\rho}}\ ;$$

i represents voight, Hill or Reuss

We have thus shown that the longitidunal propagation direction is much more important than the other two.

Anisotropy: We have calculated the longitidal and transverse propagation velocities for the TIN phase in the directions [100], [110] and [111] which we present in Table-10 with expressions of the velocities relative to the directions.

The long term propagation of the wave in the [100] direction remains the most important, while the transverse propagations [100] and [110] are equivalent and thus present the same properties, there is anisotropy. In addition to these differences, we can also note that the velocities of the long wave propagation in the [110] and [111] directions are close.

Table-9: Wave propagation speed.

Size	System								
	Voight			Reuss			Hill		
	B1	B2	B3	B1	B2	B3	B1	B2	B3
vs.	5988	4083	4432	5893	2683	4422	5940	3455	4427
vp	9761	8189	8115	9683	7378	8107	9722	7794	8111
vm	6549.5	4542.8	4897.2	6453.8	2137.9	8865.1	6501.9	3867.2	4895.2

Table-10: Speed and mode of propagation.

Direction	Mode of propagation	Expression	Value		
			B1	B2	B3
[100]	Longitudinal	$v_1 = \sqrt{C_{11}/\rho}$	10562	9538	7981
[100]	Transversal	$v_2 = \sqrt{C_{44}/\rho}$	5325	2171	4552
[110]	Longitudinal	$v_3 = \sqrt{(C_{11} + C_{12} + 2C_{44})/2\rho}$	9830	7815	8145
[110]	Transversal	$v_4 = \sqrt{C_{44}/\rho}$	5325	2171	4552
[110]	Transversal	$v_5 = \sqrt{(C_{11} - C_{12})/2\rho}$	6578	5883	4246
[111]	Longitudinal	$v_6 = \sqrt{(C_{11} + 2C_{12} + 4C_{44})/3\rho}$	9574	7149	8202
[111]	Transversal	$v_7 = \sqrt{(C_{11} - C_{12} + C_{44})/3\rho}$	6193	4965	4351

Conclusion

During this work, we used MEAM potentials for TiN alloys as well as for Ti and N elements found in the database for B1, B2 and B3 structures; the results obtained are from the LAMMPS calculation code as well as from the MPCV4 application.

We have shown that the most stable structure is the NaCl type B1 with cohesion energy of -6.62eV and a mesh parameter of 4.24A.

All modules B, G and E follow the order of magnitude such that $X_{B1} > X_{B2} > X_{B3}$ (X for module B, G, E) which is not demonstrated by the structural stability whose order of stability is given by B1>B3>B2.

The largest value of Debye temperature is observed for the Bx structure followed by By, it will be beneficial to further investigate the thermodynamic properties of these structures.

TiN is also the subject of a study on electronic properties, a study based on DFT conducted by Dr. Alain Dzabana in the research group on the physicochemical properties of materials.

References

1. J.W. He, C.D. Bai, K.W. Xu and N.S. Hu (1995). Improving the anticorrosion and mechanical behaviour of PACVD TiN. *Surf. Coatings Technol*., 74–75, (1995), 387–393.

2. Oh, S., Suh, D., & Lee, S. (1998). Microstructure of TiN/carbon steel functionally gradient materials processed by high-energy electron beam irradiation. *Materials Science and Engineering: A*, 248(1-2), 245-255.

3. Hultman, L. (2000). Thermal stability of nitride thin films. *Vacuum*, 57(1), 1-30.

4. Yu, Z., Inagawa, K., & Jin, Z. (1995). Tribological properties of TiN and TiC films in vacuum at high temperature. *Thin solid films*, 264(1), 52-58.

5. Li, J., Mayer, J. W., Shacham-Diamand, Y., & Colgan, E. G. (1992). Formation of TiN-encapsulated copper structures in a NH3 ambient. *Applied physics letters*, 60(24), 2983-2985.

6. Nicolet, M. A. (1978). Diffusion barriers in thin films. *Thin solid films*, 52(3), 415-443.

7. S. Q. Wang, I. Raaijmakers, B. J. Burrow, S. Suthar, S. Redkar and K. B. Kim (1990). Reactively sputtered TiN as a diffusion barrier between Cu and Si. *J. Appl. Phys*., 68 5176–5187.

8. M. Repeta, L. Dignard-Bailey, J.F. Currie, J.L. Brebner and K. Barla (1988). The fabrication of TiN films by reactive evaporation and rapid thermal annealing. *J. Appl. Phys*., 63, 2796–2799.

9. M. Wittmer and H. Melchior (1982). Applications of TiN thin films in silicon device technology. *Thin Solid Films*, 93, 397–405.

10. Raiteri G. and Calcatelli A. (2001). Thermal desorption from stainless steel samples coated with TiN and oxide layers. *Vacuum*, 62, 7–14.

11. Smith G.B., Swift P.D. AND Bendavid A. (1999). TiNx films with metallic behavior at high N/Ti ratios for better solar control windows. *Appl. Phys. Lett*., 75, 630.

12. Wang S., Bai X., Wang B. and Fan Y. (1996). Preparation of TiN film on brass by CAPD as a decoration system. 278, 67–73.

13. Ibrahim, M. A. M., Korablov, S. F., & Yoshimura, M. (2002). Corrosion of stainless steel coated with TiN,(TiAl) N and CrN in aqueous environments. *Corrosion Science*, 44(4), 815-828.

14. Bes, R. (2010). Comportement thermique du xénon dans le nitrure de titane fritté matrice inerte d'intérêt des RNR-G (Doctoral dissertation. Université Claude Bernard-Lyon I.

15. T. Nsongo (1987). Study by Radiofrequency and D.C Triode Sputtering of Structure and Adhesion of Titaniun and Titanium Nitride Deposed on Metallic Substrate. *Doctorate Thesis, Universite Aix- Marseill*e.

16. Grosso, S. (2017). Revêtements architecturés de Ti, TiN et TiO élaborés par pulvérisation cathodique au défilé sur des fils en acier inoxydable: relation entre la composition chimique. la microstructure et les propriétés d'usage (Doctoral dissertation, Université Grenoble Alpes).

17. Fodil, M., Mounir, A., Ameri, M., Baltache, H., Bouhafs, B., Al-Douri, Y., & Ameri, I. (2014). Structural and elastic properties of TiN and AlN compounds: first-principles study. *Materials Science-Poland*, 32, 220-227.

18. Kim, Y.-M. and B.-J. Lee (2008). Modified embedded-atom method interatomic potentials for the Ti–C and Ti–N binary systems. *Acta Materialia*, 56(14), 3481-3489.

19. Ranganathan, S. I., & Ostoja-Starzewski, M. (2008). Universal elastic anisotropy index. *Physical review letters*, 101(5), 055504.

20. Wang, A. J., Shang, S. L., Du, Y., Kong, Y., Zhang, L. J., Chen, L., ... & Liu, Z. K. (2010). Structural and elastic properties of cubic and hexagonal TiN and AlN from first-principles calculations. *Computational materials science*, 48(3), 705-709.

21. Eboungabeka, A. D., Eboungabeka Trigo, E. R. M., & Nsongo, T. (2021). Reactivity of titanium dental implants in salivary environment in the presence of foods consumed in the Republic of the Congo. *Advances in Materials Physics and Chemistry*, 11(05), 93-99.

22. Tian, J., Zhao, Y., Wang, B., Hou, H., & Zhang, Y. (2018). The structural, mechanical and thermodynamic properties of Ti-B compounds under the influence of temperature and pressure: First-principles study. *Materials Chemistry and Physics*, 209, 200-207.

23. Xiao, B., Feng, J., Zhou, C. T., Jiang, Y. H., & Zhou, R. (2011). Mechanical properties and chemical bonding characteristics of Cr7C3 type multicomponent carbides. *Journal of Applied Physics*, 109(2).

24. Mouhat, F., & Coudert, F. X. (2014). Necessary and sufficient elastic stability conditions in various crystal systems. *Physical review B*, 90(22), 224104.

25. Wang, J. H., Lu, Y., Zhang, X. L., & Shao, X. H. (2018). The elastic behaviors and theoretical tensile strength of γ-TiAl alloy from the first principles calculations. *Intermetallics*, 101, 1-7.

26. Ravindran, P., Fast, L., Korzhavyi, P. A., Johansson, B., Wills, J., & Eriksson, O. (1998). Density functional theory for calculation of elastic properties of orthorhombic crystals: Application to TiSi 2. *Journal of Applied Physics*, 84(9), 4891-4904.

27. Ledbetter, H., & Migliori, A. (2006). A general elastic-anisotropy measure. *Journal of applied physics*, 100(6).